



The key role of atmospheric absorption in the Asian Summer Monsoon response to dust emissions in CMIP6 models

Alcide Zhao^{1,2}, Laura J. Wilcox^{1,2}, Claire L. Ryder¹

5 ¹Department of Meteorology, University of Reading, Reading, UK

²National Centre for Atmospheric Science, UK

Correspondence to: Claire L. Ryder (c.l.ryder@reading.ac.uk)

Abstract.

We investigate the Asian Summer Monsoon (ASM) response to global dust emissions in the Coupled Model Intercomparison
10 Project Phase 6 (CMIP6) models, which is the first CMIP to include an experiment with a doubling of global dust emissions
relative to their preindustrial levels. Thus, for the first time, the inbuilt influence of dust on climate across a range of climate
models being used to evaluate and predict Earth's climate can be quantified. We find that dust emissions cause a strong
atmospheric heating over Asia that leads to a pronounced hemispheric energy imbalance. This results in a surface cooling over
Asia, an enhanced Indian Summer Monsoon and a southward shift of the Western Pacific Intertropical Convergence Zone (ITCZ)
15 which are consistent across models. However, the East Asian Summer Monsoon response shows large uncertainties across
models, arising from the diversity in models' simulated dust emissions, and in the dynamical response to these changes. Our
results demonstrate the central role of dust absorption in influencing the ASM, and the importance of accurate dust simulations
for constraining the ASM and the ITCZ in climate models.

1 Introduction

20 Mineral dust is the most abundant aerosol type by mass in the Earth's atmosphere (Kok et al., 2018; Gliss et al., 2021), and
their emissions have at least doubled since preindustrial times (Hooper and Marx, 2018). Dust aerosols play an important role
in the Earth's radiation balance and climate system by interacting with radiation, clouds, and ecosystems during its life cycle
(Carslaw et al., 2010; Mahowald et al., 2010; Kok et al., 2018; Chaibou et al., 2020; Jin et al., 2021). Overall, dust serves as a
cooling agent at the top of the atmosphere (TOA) over all but the brightest surfaces (Chaibou et al., 2020). Dust also heats the
25 atmospheric column by absorbing solar radiation but also cools the atmosphere through terrestrial radiation interactions,
thereby perturbing the vertical temperature profile (Balkanski et al., 2021; Ryder, 2021). However, our knowledge of dust-
climate interactions, including the magnitude and sign of dust's radiative effect, remains highly uncertain due to incomplete
understanding of its physical and chemical properties (Formenti et al., 2011; Richter and Gill, 2018; Di Biagio et al., 2019;
Adebiyi and Kok, 2020), life cycles (Shao et al., 2011; Kok et al., 2021b; Wu et al., 2020), and interactions with other



30 components of the Earth system (Karydis et al., 2017; Chaibou et al., 2020; Li et al., 2021), as well as the challenges of incorporating these processes into models.

Present-day global dust emissions are confined primarily to the Northern Hemisphere tropical and subtropical regions (i.e., the so-called dust-belt (Shi et al., 2021)), with around 30-40% emitted from the Asian source regions (Kok et al., 2021a). There are numerous studies investigating Asian dust-climate interactions, and particularly their links to the Indian Summer Monsoon (ISM) (Sun et al., 2012; Chen et al., 2017; Wang et al., 2020; Jin et al., 2021). It is found that dust impacts the ISM through many different pathways including the elevated heat pump mechanism (Lau et al., 2006), snow-darkening feedbacks (Sarangi et al., 2020), and dust-cloud interactions (Karydis et al., 2017). However, most of these mechanisms are model-based and are subject to large uncertainties in model physics and parameters (Jin et al., 2021). Unfortunately, these uncertainties are very difficult to constrain using available observations. Compared to the ISM, there are larger uncertainties in our understanding of the interactions between dust and the East Asian climate, including the East Asian Summer Monsoon (EASM) (Sun et al., 2012; Chen et al., 2017; Wang et al., 2020). Dust emissions have the potential to impact both the ISM and the EASM, collectively known as the Asian Summer Monsoon (ASM).

45 The availability of the Coupled Model Intercomparison Project Phase 6 (CMIP6; Eyring et al. (2016)) experiments offer a great opportunity to understand the climate impacts of dust emissions and the role dust plays in the latest generation of climate models. Zhao et al. (2022) examined the global and regional simulation of dust in 16 CMIP6 models in the Atmospheric Model Intercomparison Project (AMIP) experiments compared to observations and reanalyses, finding that most models captured features such as spatial distribution and seasonal cycles of dust well, but found dust emission and deposition to be poorly represented, and found that the ranges of simulated dust burden and optical depth across models are larger than that of previous model generations. Several publications have examined dust simulation and response to climate change in other CMIP6 experiments. Aryal and Evans (2021) examined dust sensitivity to drought in historical and future SSP585, showing that soil moisture is a better indicator of dust variability than precipitation, highlighting the importance of the land surface in simulating the dust cycle accurately. Aryal and Evans (2023) and Zhou et al. (2023) explored the response of dust emissions and surface concentrations to temperature and precipitation/soil moisture changes, finding substantial regional variability. Zhao et al. (2023) found that overall, dust loading increases globally by the end of the twenty-first century in CMIP6 model simulations, though this is dependent on the future scenario and region, with East Asia and the western Pacific showing decreasing dust load due to increasing precipitation in these regions. Contrastingly, Mao et al. (2021) suggest an increase in East Asian dust emissions in CMIP6 future simulations due to enhanced frequency of circulation patterns connected to extreme dust events. Li and Wang (2022) explored drought-dust relationships over the southeastern USA in CMIP6 historical simulations.

The CMIP6 Aerosols and Chemistry Model Intercomparison Project (AerChemMIP; Collins et al. (2017)) has for the first time included a doubled-dust experiment alongside single forcing experiments with other aerosol species. This allows us to



consistently isolate and quantify the impacts of dust emissions in multiple state-of-the-art climate models. Although dust
65 aerosols have been included in previous CMIP experiments as well as the latest CMIP6 historical, AMIP and future SSP
experiments, these experiments do not allow the isolation of the specific effect of dust on radiation and climate in a multi-
model context. It is important to understand the role and extent of dust in impacting climate in the CMIP6 simulations, where
the effects of dust on climate (through mechanisms such as surface, atmospheric or top of atmosphere radiative effects and
subsequent complex impacts on atmospheric circulation) are not explicit. For the first time, the new AerChemMIP experiments
70 allow this to be diagnosed.

We present a multi-model study to determine the atmospheric response to a change in global dust emissions in Asia based on
two sets of the AerChemMIP simulations from seven CMIP6 models (Section 2). Dust radiative forcing, temperature, and
precipitation responses, as well as the circulation changes and mechanisms are presented in Section 3. Our major findings and
75 their implications are summarised in Section 4.

2 Models and Simulations

To explore the impact of dust emissions, we used two sets of time-slice simulations from seven participating CMIP6 models
shown in Table 1, which provided dust diagnostics. We include all 7 models regardless of how well (or poorly) they represent
the dust cycle (Zhao et al., 2022), in order to firstly understand the implicit effect of dust in climate simulations in general
80 within CMIP6 models, and secondly to avoid limiting further the number of models analysed. Even if models do not simulate
the dust cycle well, it is important to understand how dust may be influencing the climate and circulation in CMIP6 models.
The base simulation (piClim-control) has all forcings fixed at preindustrial (year 1850) levels. The AerChemMIP perturbation
simulation (piClim-2xdust) is identical to piClim-control except that dust emissions are doubled globally. The CMIP6 models
reproduce major features of global dust processes well (Zhao et al., 2022), including the spatial patterns of global dust
85 emissions and dust aerosol optical depth (DOD). Dust emissions were calculated online in all the seven models in piClim-
control, and were doubled in piClim-2xdust by either scaling the dust emission parameterisations or the emission data files
(Collins et al., 2017). As such, we define the climate impacts of dust emissions as the difference between piClim-2xdust and
piClim-control (i.e., piClim-2xdust minus piClim-control). Sea surface temperatures and sea ice distributions were prescribed
as 1850 climatological averages in both simulations. Therefore, the responses presented here represent the fast response of the
90 climate system due to rapid adjustments of the atmosphere to changes in energy balance as a direct result of dust emissions
(Ganguly et al., 2012; Samset et al., 2016; Zanis et al., 2020). Dust can be activated as cloud condensation nuclei in all models
except CNRM-ESM2-1 and UKESM1-0-LL, while two models (NorESM2-LM and MPI-ESM-1-2-HAM) have parameterized
dust particles also acting as ice nuclei.



Model	Variant label	Resolution (lon × lat × Lev)	Model years	Dust size diameter boundaries (µm)	Dust as CCN/IN	Global JJA mean effective radiative forcing (W m ⁻²)	References
CNRM-ESM2-1	r1i1p1f2	1.4° × 1.4° × 91L	30	3 bins (0.01-1.0, 1.0-2.5, 2.5-20)	N/N	0.08	Séférián et al. (2019)
GFDL-ESM4	r1i1p1f1	1.25° × 1° × 49L	30	5 bins (0.2-2, 2-4, 4-6, 6-12, 12-20)	Y/N	-0.07	Dunne et al. (2020)
GISS-E2-1-G	r1i1p3f1	2.5° × 2° × 40L	41	6 bins (<1, 1-2, 2-4, 4-8, 8-16, 16-32)	Y/N	-0.11	Kelley et al. (2020)
IPSL-CM6A-LR-INCA	r1i1p1f1	1.25° × 1.27° × 79L	30	1 lognormal mode with mass median diameter (geometric standard deviation): 2.5 (2)	Y/N	-0.19	Di Biagio et al. (2020)
MPI-ESM-1-2-HAM	r1i1p1f1	1.875° × 1.875° × 47L	40	2 modes with median particle radii boundaries: 0.005-0.05 and >0.05	Y/Y	-0.13	Neubauer et al. (2019); (Tegen et al., 2019)
NorESM2-LM	r1i1p1f1	2.5° × 1.875° × 32L	30	Three modes: Aikten: 0.01-0.1; Accumulation: 0.1-1.0; Coarse: 1.0-10.0	Y/Y	0.04	Kirkevåg et al. (2018)
UKESM1-0-LL	r1i1p1f4	1.875° × 1.25° × 85L	45	6 bins :0.064-0.2, 0.2-0.63, 0.63-2.0, 2.0-6.32, 6.32-20, 20-63	N/N	0.13	Mulcahy et al. (2020)

95 **Table 1: Details of CMIP6 models used in this study**

For each model and experiment, a simulation of at least 30 years is available. All model data are interpolated to a 2x2-degree horizontal grid when computing the multi-model mean (MMM). We focus on the response over Asia (box in Figure S1f) in the summertime (June-July-August; JJA) when the Asian Summer Monsoon (ASM) is fully established (Li et al., 2016; Zhao et al., 2019; Jin et al., 2021). Note all the changes presented here are due to a doubling of global dust emissions, and we refer to this as ‘dust emissions’ for simplicity.



We diagnosed the dust effective radiative forcing (ERF) as the differences in net radiative fluxes between piClim-2xdust and piClim-control at the top-of-the-atmosphere (TOA) and at the surface (Forster et al., 2016). We then defined change in atmospheric absorption due to dust emissions as the difference between TOA and surface ERF. The response to dust emissions such as changes in surface temperature and precipitation are calculated as averages of JJA means of the last 30 years of each simulation (Table 1). We tested the statistical significance of the response at the $p \leq 0.1$ confidence level using the Monte-Carlo test. We have also identified regions where there are inconsistent responses across models, defined as regions where ≤ 4 of the 7 models have the same sign as the MMM. Radiative fluxes are given as total (shortwave plus longwave) unless specifically stated otherwise.

3 Summertime climate responses to dust emissions

The models' simulated changes in dust emissions and DOD are shown in Figure 1, while the JJA climatologies of DOD, precipitation, 850-hPa winds and sea level pressure fields are included in Supplement Figures S1-S4 for reference. We note the large diversities in models' simulated dust climatology (Figure 1, S1), and hence in the changes to DOD (Figure S4) because of doubling global dust emissions. Such inter-model diversities are most pronounced over the Chinese deserts and East Asia where a half of the models simulate very little dust emission. The models also simulate very different monsoon climatologies (Figure S2, S3), which will contribute to differences in the DOD distribution through dust transport and wet deposition differences, and likely to differences in the response of the monsoon to the dust forcing (Liu et al., 2018).

120

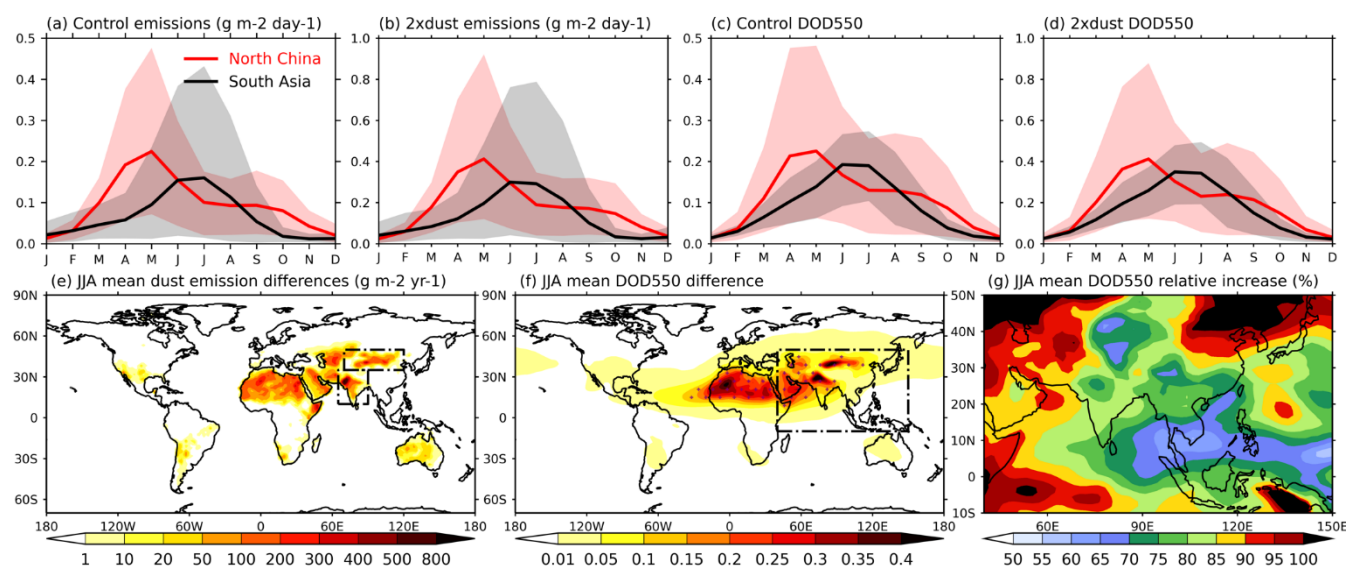


Figure 1: Model simulated (30-year mean) seasonal cycles of (a, b) dust emissions ($\text{g m}^{-2} \text{ day}^{-1}$) and (c, d) DOD at 550 nm (DOD550) over the Chinese desert (red) and South Asia (black; see boxes in (e)) in (a, c) piClim-control and (b, d) piClim-2xdust. Shadings represent the 5th-95th percentiles of the multi-model ensemble spread. Maps show multi-model mean of JJA mean differences in (e) dust emissions ($\text{g m}^{-2} \text{ yr}^{-1}$), (f) DOD550, (g) the multi-model mean of percentage increase in DOD550 relative to the piClim-Control

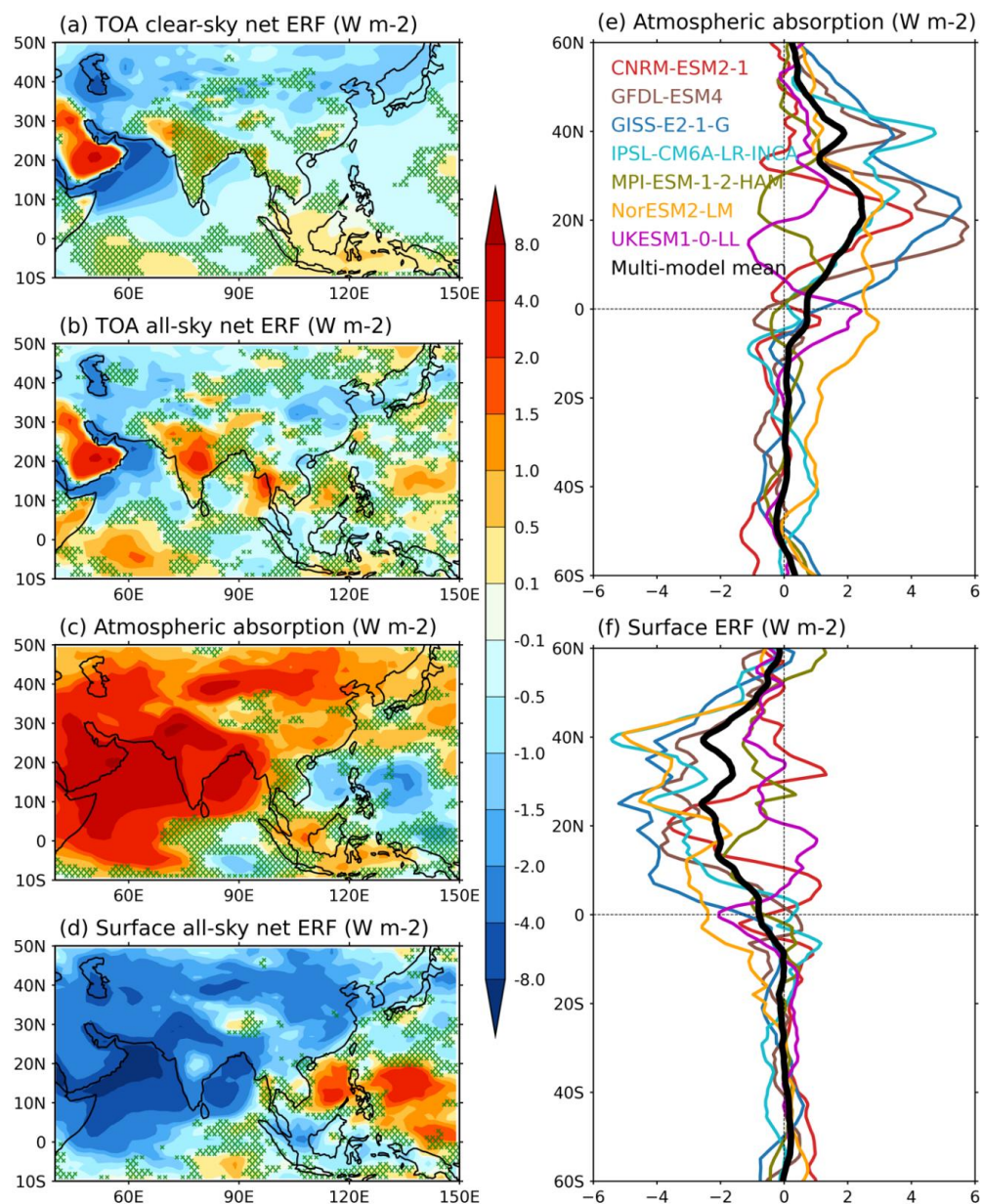
125



climatology over Asia (denoted by box in (f)). Purple hatches in (f) denote statistical insignificance at the 10% level of the multi-model mean DOD changes.

3.1 Changes in radiative forcing and clouds

130 Figure 2 shows the spatial patterns, and zonal mean profiles, of the ERF over Asia due to dust emissions. Those for individual models can be found in Figures S5-S9. The clear-sky ERF at TOA in the MMM shows a general negative forcing (Figure 2a) due to the direct dust-radiation interactions (i.e., scattering and absorption). There is however a positive clear-sky TOA ERF pattern that is confined over the bright surface of the Arabian Peninsula, as well as over South and Southeast Asia (particularly in CNRM-ESM2-1, GFDL-ESM4 and UKESM1-0-LL; Figure S6). The spatial pattern of all-sky TOA ERF in the MMM (Figure 2b) resembles that of clear-sky over the land, yet large differences exist across models (Figure S6). Over South Asia, 135 all models but IPSL-CM6A-LR-INCA (-1.73 W m^{-2}) simulate a positive TOA ERF ($0.01\text{-}3.38 \text{ W m}^{-2}$) due to dust induced atmospheric absorption (Figure 1c) and cloud increases (Figure 2a, c).



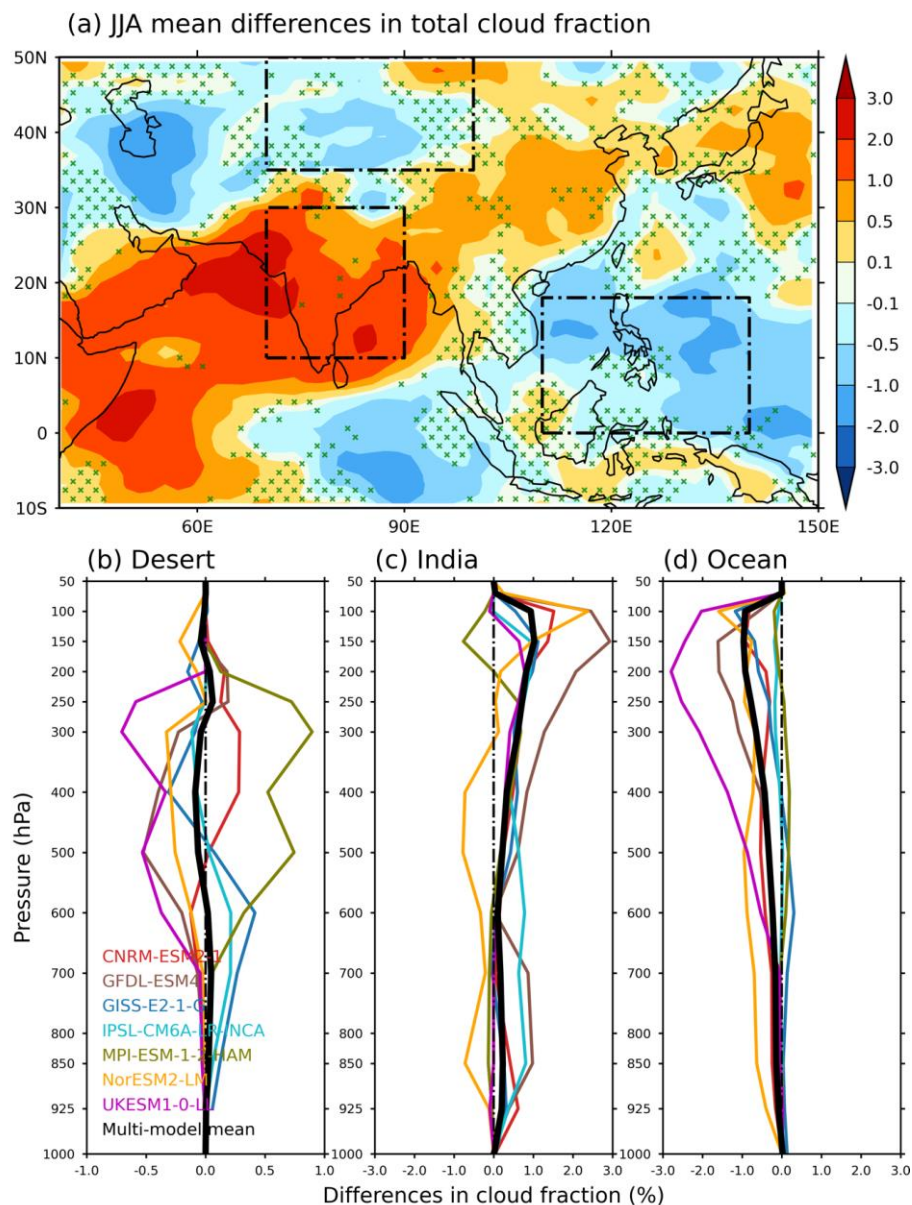
140 **Figure 2:** JJA mean changes in radiative fluxes (W m^{-2}) due to doubled dust emissions. Maps show multi-model mean differences in (a) clear-sky effective radiative forcing (ERF) at the top-of-the-atmosphere (TOA), (b) TOA all-sky net ERF, (c) all-sky atmospheric total (shortwave plus longwave) absorption, and (d) surface all-sky net ERF. Green hatches denote where ≤ 4 models have the same sign as the multi-model mean. Curves show the zonal mean differences in (e) net atmospheric absorption and (f) surface ERF averaged between 40°E - 150°E . Coloured curves represent individual models and black curves the multi-model mean.

145 Dust emissions result in significant atmospheric heating through dust absorption above land and the Arabian Sea (Figure 2c). The heating is robust across almost all models (Figure S7), producing a MMM of 1.58 (0.23 - 2.94) W m^{-2} over Asia (box in



Figure 1f), which is dominated by the shortwave radiative heating (Figure S8a) that is partially cancelled out by the longwave radiative cooling (Figure S8b). The atmospheric heating is particularly prominent over South Asia (4.28 (1.01-9.59) W m⁻²). As a result of the dust-induced atmospheric absorption, there is a pronounced negative surface ERF over land, contrasting with the positive surface ERF over the Tropical Western Pacific Ocean (Figure 2d, S9). The positive surface ERF over the ocean is attributable to reductions in clouds (Figure 3, d) that allow more solar radiation to reach the surface.

Changes in the spatial pattern of total cloud fraction (Figure 3a, S10) over Asia, and especially over South Asia (0.26%-3.49%), show robust common patterns across models except MPI-ESM-1-2-HAM (-0.37%). All models show that such changes come from high cloud changes (above 200 hPa) over the Indian subcontinent (Figure 3c), the Arabian sea, the Pacific Ocean (Figure 3d), and East China (not shown), and changes in mid-level clouds (700-200 hPa) above the Chinese deserts (Figure 3b). The cloud changes over South Asia and the Pacific Ocean are associated with changes in the large-scale atmospheric circulation (Section 3.3) rather than increases in dust which may modify cloud microphysical properties (not shown).



160 **Figure 3: JJA mean changes due to doubled dust emissions in (a) multi-model mean of total cloud fraction (%) and (b-d) vertical profiles of cloud fraction averaged within the three boxes in (a). Coloured curves represent individual models, and black the multi-model means. Green hatches in (a) denote where ≤ 4 models have the same sign as the multi-model mean.**

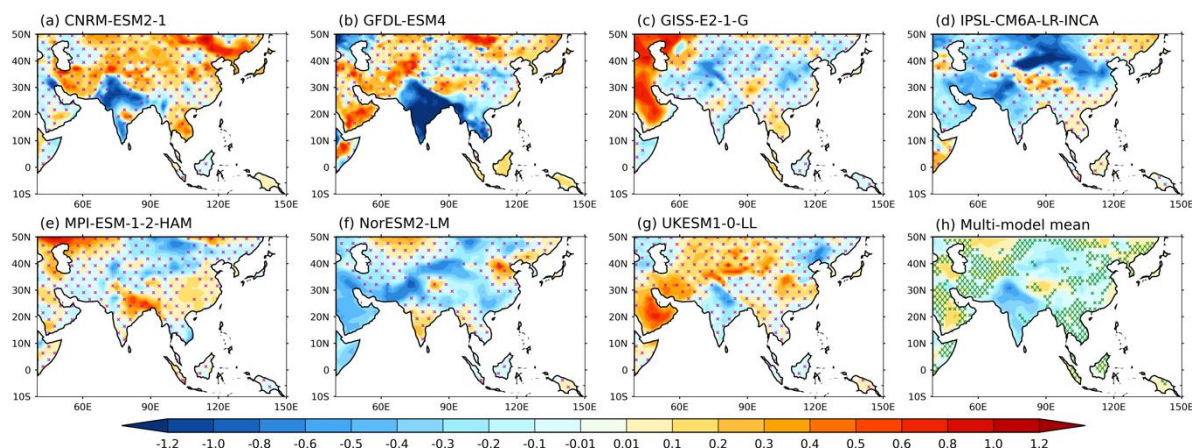
165 The dust-induced atmospheric absorption leads to a hemispheric asymmetry in energy distributions, as demonstrated by the changes in the Asian zonal mean atmospheric absorption (Figure 2e) and surface ERF (Figure 2f). The asymmetry is pronounced over the dustiest regions between 40E and 100E, encompassing the Arabian Peninsula, The Middle East, India



and the Taklamakan desert, and is weaker over the East Asia-Western Pacific region. We show in Sections 3.3 that such asymmetry has important fingerprints on dust-induced precipitation and circulation changes.

3.2 Temperature Response

Figure 4 shows JJA mean near-surface temperature changes in response to dust emissions. The temperature response is characterised by a cooling of the Indian subcontinent (-0.17 K) and the Chinese desert regions (-0.12 K) in the MMM (Figure 4h). The cooling is consistent across most models and is the largest in GFDL-ESM4 over India (up to -1.8 K), and in IPSL-CM6A-LR-INCA over the Chinese deserts (around -1.05 K). However, models disagree markedly with each other about the pattern, and even the sign, of the temperature responses over other regions such as Central Asia, East Asia and the Arabian Peninsula. Over these regions, as opposed to the cooling seen in other models, the CNRM-ESM2-1 (Figure 4a), MPI-ESM-1-2-HAM (Figure 4e), and UKESM1-0-LL (Figure 4g) models simulate wide-spread warming. These models are also the ones with the lowest DOD climatology (Figure S1) and simulate the smallest DOD changes (Figure S4) there amongst the seven models. This uncertainty demonstrates the crucial importance of better observationally constrained representation of dust processes in climate models for simulating the dust-climate interactions.



180 **Figure 4: JJA mean changes in near-surface temperature due to doubled dust emissions in (a-f) individual models and (h) the multi-model mean. Purple hatches indicate lack of statistical significance at the 10% level. Green hatches in (h) denote where ≤ 4 models have the same sign as the multi-model mean.**

The temperature responses in individual models do not follow the dust ERF at TOA (Figure 2b, S6), which shows opposite signs over some regions such as India. In comparison, near-surface temperature responses show better, yet weak, agreement with surface ERF patterns (Figure 2d, S9). These imply the central role of dust-radiation interactions in changing the surface radiation budget and temperature. However, as discussed in the following section, the effects of dust-radiation interactions do not fully explain changes in near-surface temperature and the large differences across models.

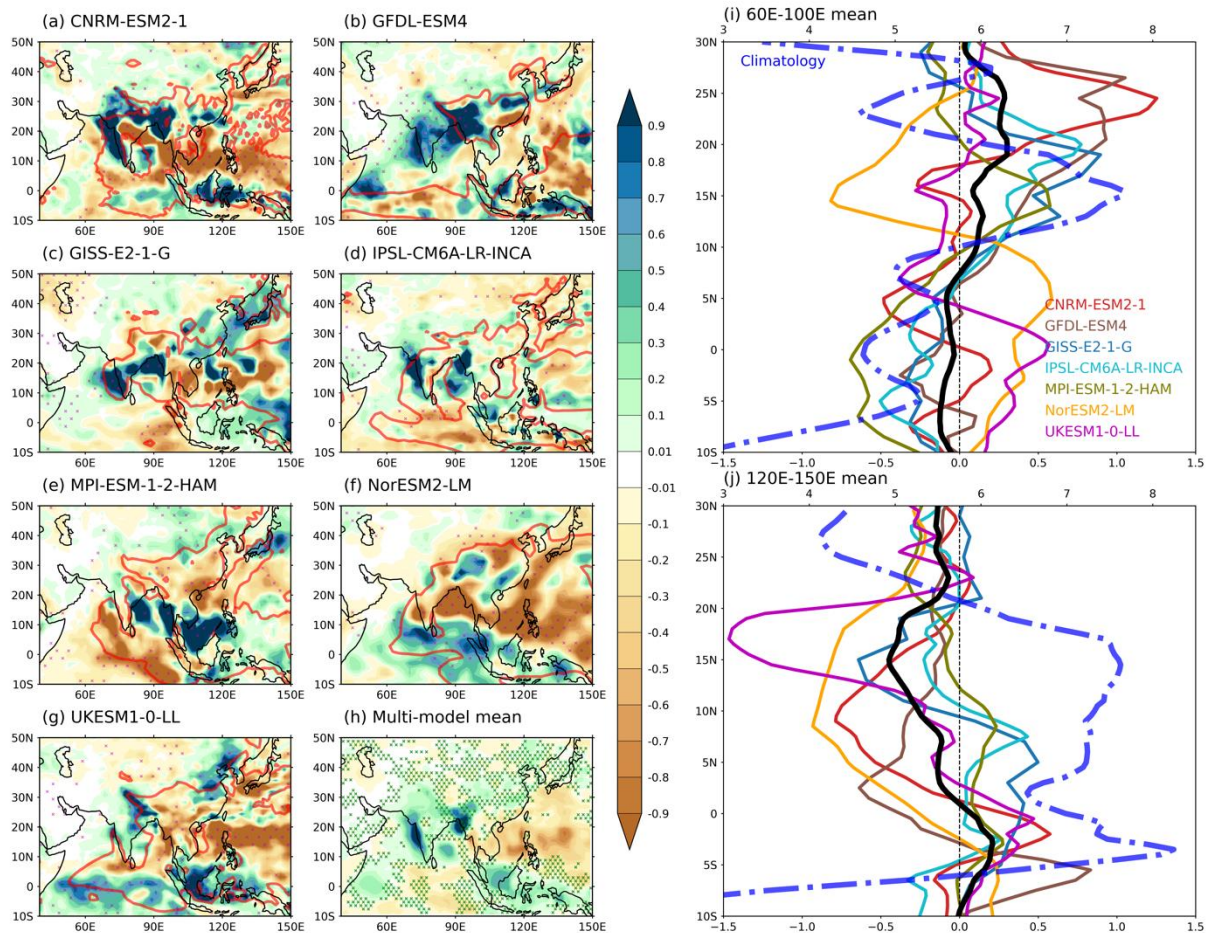


Overall, dust emissions result in a general surface cooling of the Asian continent in most models. However, there are significant diversities in model-simulated pattern and sign of temperature changes, despite the relatively consistent changes in cloud and radiation across models. Such diversity is only partly explained by the diversity in the models' simulated dust climatologies. Meanwhile, we show below that such diversity in surface temperature response is also intertwined with changes in precipitation and monsoonal circulation.

3.3 Precipitation and circulation responses

In this section, we turn to JJA mean changes in precipitation due to dust emissions while attempting to understand the underlying mechanisms by examining changes in the ASM.

Figure 5 shows the spatial patterns, as well as the zonal mean profiles over the South Asia region (60-100°E, Figure 5i) and the East Asia-Western Pacific region (120-150°E, Figure 5j), of precipitation changes in response to dust emissions. We note that large uncertainties in models' simulated precipitation changes are expected due to challenges in simulating the ASM (Wilcox et al., 2020; Wang et al., 2021) in addition to the diversity of the dust climatologies. Nevertheless, the precipitation responses exhibit certain common robust features. Particularly, the increased precipitation over the Indian subcontinent and Southeast Asia (i.e., Indonesia and Papua New Guinea south of the Equator), as well as the drying of the Western Pacific Ocean.



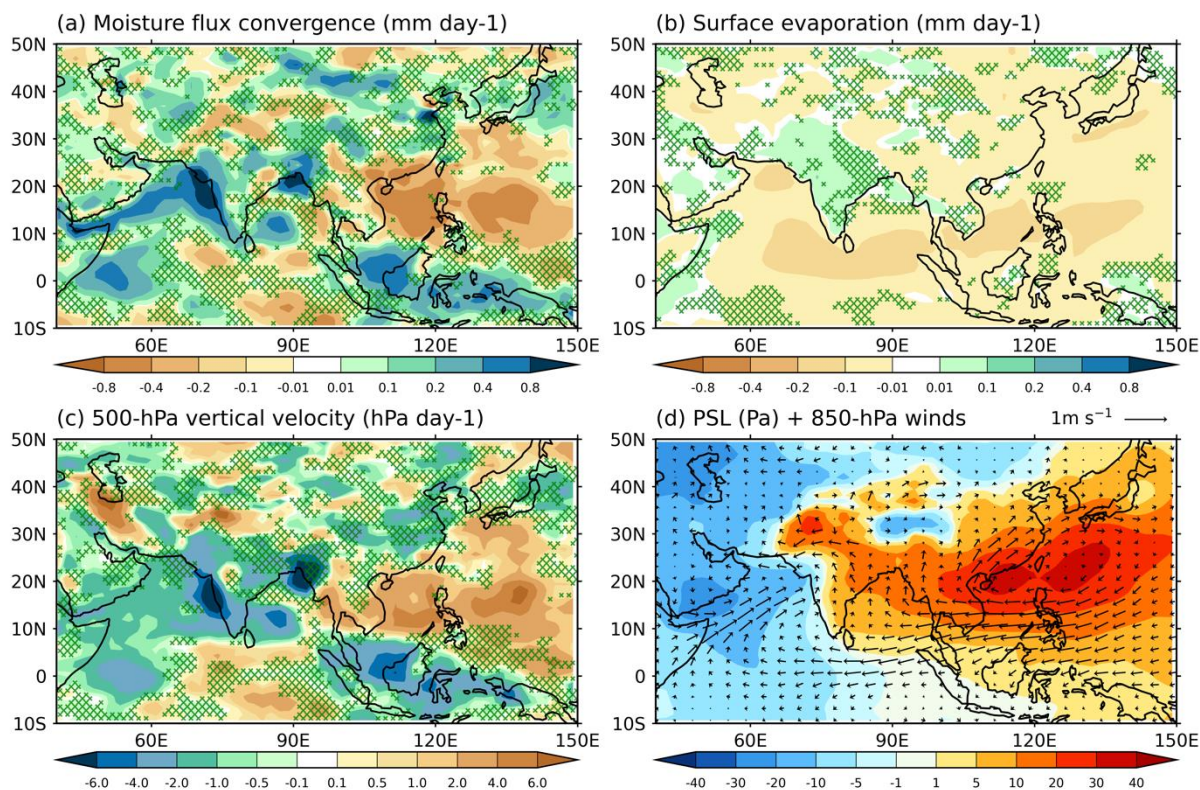
205

Figure 5: JJA mean changes due to doubled dust emissions in precipitation (mm day^{-1}) in (a-f) individual models and (h) the multi-model mean. Red contours in (a-g) represent the 5 mm day^{-1} JJA climatology derived from piClim-Control. Purple hatches indicate lack of statistical significance at the 10% level. Green hatches in (h) denote where ≤ 4 models have the same sign as the multi-model mean. Curves show the JJA zonal mean changes in precipitation (mm day^{-1}) averaged between (i) 60°E - 100°E and (j) 120°E - 150°E . Coloured curves represent individual models, black curves are multi-model means, and the blue dashed curves show JJA climatology derived from piClim-Control.

210

215

The MMM precipitation response (Figure 5h) is largely explained by changes in the vertically integrated moisture flux convergence (Figure 6a), whilst there is very little contribution from local convective processes, as demonstrated by the very limited changes in surface evaporation (Figure 6b). These, along with consistent changes in the 500-hPa vertical velocity (Figure 6c), demonstrate the predominant role of large-scale atmospheric circulation changes in shaping the fast precipitation response to dust emissions. The above is justified by careful comparisons of these fields (Figures S11-S12) to precipitation changes (Figure 5) in each individual model. For example, the pattern of precipitation increases over the Indian subcontinent match well with the anomalous 500-hPa ascent and moisture convergence in most models. In comparison, the drying of the western Pacific Ocean is accompanied by strong anomalous descent at 500-hPa and moisture divergence in all models.



220

Figure 6: JJA multi-model mean changes due to doubled dust emissions in (a) vertically integrated moisture flux convergence (mm day^{-1}), (b) surface evaporation (mm day^{-1}), (c) 500-hPa vertical velocity (hPa day^{-1} ; negative values indicate increased upward motion), and (d) sea level pressure (colour; Pa) overlaid with 850-hPa winds (vector; m s^{-1}). Green hatches denote where ≤ 4 models have the same sign as the multi-model mean.

225

The zonal mean precipitation changes show an enhancement of the ISM, with precipitation increasing over land and decreasing over the equatorial Indian Ocean in most models. That is, a northward shift of the rain belt over the ISM region (Figure 5, Figure 6). This is supported by changes in the 850-hPa winds in the MMM (Figure 6d) and in most models (Figure S13). Extensive lower tropospheric anti-cyclonic and south-westerly anomalies bring extra moisture from the Arabian Sea to the land. Over the Bay of Bengal, there are however anomalous southerlies that impede the climatological westerly flows; such southerlies are consistent with the pattern of enhanced precipitation there. The monsoonal precipitation increases lead to further cooling of the Indian subcontinent on top of the dust induced radiative surface cooling (Figure 4). The above changes in MMM are also seen in most individual models. However, two models (MPI-ESM-1-2-HAM and NorESM2-LM) simulate weakened ISM circulation. This is consistent with the precipitation reduction over the Indian subcontinent (Figure 5e, f) and explains the model-simulated warming there (Figure 4e, f) in these two models.

230
235



The importance of dust induced atmospheric absorption in changing the ISM and precipitation has been studied extensively (Maharana et al., 2019; Wang et al., 2020; Bercos-Hickey et al., 2020; Cruz et al., 2021; Jin et al., 2021; Balkanski et al., 2021), with several different physical mechanisms proposed to explain their interactions. For example, snow darkening effects (Sarangi et al., 2020) and the elevated heat pump (EHP) mechanism (Lau et al., 2006). Here we found that dust emissions cause enhanced atmospheric absorption over the Arabian Sea and South Asia (Figure 2) which is linked to enhanced moisture flux convergence via adjustments in circulations, and therefore an enhancement in the ISM in most models (Figure 6d). The enhanced ISM draws moisture from the oceans to the northern Indian subcontinent (Figure 6c), producing anomalous ascent and precipitation (Figure 5h), as well as collocated increases in high clouds (Figure 3). At the same time, strong southwesterlies within the monsoon are likely to transport more dust from the Arabian Peninsula to the Arabian Sea and Northern India. In doing so, the ISM is further enhanced through the EHP feedback loop brought about by the enhanced upper-tropospheric meridional temperature gradient because of increases in dust absorption.

The East Asian Summer Monsoon (EASM) presents a mixed response (Figure 6d) to dust emissions. A westward extension of the West Pacific Subtropical High results in an enhanced monsoon flow over eastern China, and strong easterly anomalies over the tropical western Pacific Ocean and the South China Sea. The easterly anomalies disrupt the climatological north-eastward transport of moisture flux from the oceans to the land (Figure S11). As a result, precipitation decreases over Southern China land areas, and only increases moderately over Northeast China in a few models (GFDL-ESM4, GISS-E2-1-G and UKESM1-0-LL) despite the enhanced monsoonal circulation over land. This demonstrates the large inter-model uncertainty in the response of the EASM to dust emissions in CMIP6 models that underpins the small response in the MMM. Such uncertainties can be attributed to several factors including model deficiencies in simulating the EASM (Wilcox et al., 2015), the mixed circulation changes due to dust emissions, as well as the very low dust emissions over East Asia in most models.

The East Asia-Pacific region sees a southward shift of the Western Pacific ITCZ that is robust across models (Figure 5j). The southward shift of the Western Pacific ITCZ can be also seen in the spatial patterns of precipitation changes that feature a north-south (drying centred around 15°N versus wetting centered around 5°S) dipole. The Western Pacific ITCZ shift is consistent with the dust-emission-induced hemispheric asymmetry (i.e., a cooler Northern Hemisphere) in surface radiative forcing (Figure S9) due to atmospheric absorption (Figure 2c, f). This is consistent with Evans (2020) who found a linear relationship between dust emissions-induced hemispheric asymmetry in radiative forcing and tropical precipitation shift along global ITCZs. The southward shift of the Western Pacific ITCZ is accompanied by a general expansion of the Western Pacific Hadley circulation and an enhancement of its ascending branch (not shown), as well as anomalous descent over the subtropical Western Pacific Ocean (Figure 6c, S12). The regions of anomalous descent are associated with collocated reductions in cloud fraction (Figure 3), anomalous surface high pressure (Figure 6d, S13), moisture divergence (Figure 6c, S11), and precipitation reduction (Figure 5). The equatorward limbs of the moisture divergence feed the Hadley circulation, forming a positive feedback loop between the drying of the subtropical Western Pacific Ocean and the southward shift of the Western Pacific

ITCZ. The regions of anomalous moisture divergence in some models also feed the tropical/subtropical anomalous easterlies that partly explain the mixed response of the EASM circulations.

275 Overall, we found a mixed response of the ASM to dust emissions which shows considerable diversity across models. The inter-model diversity in the atmospheric circulation response to dust is reflected in the uncertainties in models' simulated temperature and precipitation changes. Nevertheless, the presence of a number of robust circulation changes across the models, and the fact that precipitation changes closely follow changes in circulation changes and moisture convergence, reveal the importance of large-scale atmospheric circulation changes in shaping temperature and precipitation responses induced by dust emissions. The impact of dust on the ASM suggests that deficiencies in ASM model simulations in general may be associated
280 with the representation of dust processes. Meanwhile, the links between the shift of the Western Pacific ITCZ and dust may have implications for the poorly constrained global ITCZs in most climate models (Samanta et al., 2019; Fiedler et al., 2020; Mamalakis et al., 2021). Specifically, since most models fail to capture the interannual to interdecadal variabilities of global and regional dust processes (Wu et al., 2019; Jin et al., 2021; Evan et al., 2014), they may also fail to reproduce the fingerprint of dust on the variability of global and regional ITCZs and monsoon systems on a number of timescales.

285 **4 Conclusion and Discussion**

We investigated the fast ASM response to a doubling of global dust emissions in seven CMIP6 models. Our results offer a parallel to the impacts of preindustrial to present-day global dust emission changes since global dust emissions have approximately doubled since preindustrial times, as well as an insight into the concealed effect of dust on climate within the latest generation of climate models. We found that doubled dust emissions cause significant atmospheric absorption, which
290 exhibits hemispheric asymmetry, consistent with the asymmetry in emissions. This results in the cooling of the Indian subcontinent, the intensification of the ISM despite the surface cooling, and the southward shift of the Western Pacific ITCZ. These demonstrate important fingerprints of dust emissions on the ASM through dust absorption-induced large-scale circulation changes. However, there are considerable uncertainties in models' simulated dust processes and in the large-scale circulation changes in response to dust emissions across models. Particularly, the model climatology of dust emission and
295 loading seems to play a role in model-simulated climate responses; it is difficult to investigate such relationships using the models and experiments currently available. Nevertheless, this demonstrates the importance of observationally constrained dust processes and properties, particularly absorption, for constraining the ASM, and better constrained large-scale circulations for more reliable simulations of dust-climate interactions.

300 We provide the caveat that the responses to dust emissions might be incomplete in the model simulations we analysed here (Zanis et al., 2020). First, changes in atmospheric circulation could change dust emissions that are not fully considered in all models by the piClim-2xdust experiment, which means the coupling between dust emissions and climate and the associated

feedbacks are not fully realised in all model simulations. Second, the CMIP6 models poorly capture and underestimate dust load over the Indian subcontinent (Zhao et al., 2022). Therefore, the dust induced atmospheric absorption there might also be underrepresented. Third, the contribution of Asian dust emissions to the global total is found to be underestimated by present generation climate models (Kok et al., 2021a). Fourth, the significant low biases in the size and size distributions of dust particles in present generation climate models (Ryder et al., 2019; Adebisi et al., 2023; Huang et al., 2021) may also mean underestimated atmospheric absorption and reduced longwave dust-radiation interactions. However, recent results (Di Biagio et al., 2019) suggest that climate models tend to apply values of the imaginary part of the refractive index of dust which are too high in the shortwave spectrum, which may counteract omitted shortwave absorption from coarse dust to some extent in some models. In fact, radiation changes induced by dust are sensitive to factors including single-scattering albedo, mass extinction coefficient, and asymmetry factor (Hatzianastassiou et al., 2004; Solmon et al., 2008; Papadimas et al., 2012; Strong et al., 2015). Additionally, these parameters are sensitive to the modelled size-resolved mass concentration, data for which is generally not available for the CMIP experiments. Inclusion of such data in future CMIP experiments would be beneficial for understanding the breadth of interactions from dust optical properties through to climate and circulation, and is recommended for inclusion in future experiments. Therefore, assumptions and uncertainties around these parameters in climate models will have great implications for model-simulated signs and magnitudes of the climate responses to dust emissions. Finally, the experiments analysed here are atmosphere-only simulations. The pattern and magnitude of the response to dust is likely different in fully-coupled climate models, as has been demonstrated in several studies of the response to anthropogenic aerosols (Ganguly et al., 2012; Samset et al., 2016; Voigt et al., 2017), since the anticipated cooling effect of dust on sea surface temperatures may have impacts on monsoon circulation.

We acknowledge that the climate response to dust emissions are still highly uncertain in climate models, given the large diversity reported here. However, whether conclusions drawn from the seven models analysed here are just a reflection of a sample of many more CMIP6 models is unknown. This warrants a community effort to better understand and simulate dust processes in climate models given their potential significance in accurately simulating other intertwined processes. The responses presented here are due to global dust emissions, and we recommend further model experiments to compare the impacts of local vs. remote dust emissions. Dust as ice nuclei and related processes are still missing in most models, which may affect model-simulated dust-climate interactions (Froyd et al., 2022). We noted however that two models (MPI-ESM-1-2-HAM and NorESM2-LM) have parameterised dust particles as ice nuclei. Nonetheless, changes in ice-cloud microphysics (not shown) in these two models are insignificant and do not explain their differences compared to other models. We therefore suggest further studies to understand the possible reasons behind this.

In summary, we found that doubling global dust emissions results in a cooling over much of Asia, an enhanced ISM and precipitation over Indian subcontinent, a mixed response of the EASM, and a southward shift of the Western Pacific ITCZ in the CMIP6 models. However, these responses feature large inter-model diversities that are intertwined with diversities in



340 model-simulated large-scale circulation changes mediated by atmospheric absorption. These responses may only represent a certain fraction of the full response. It is therefore possible that dust may play an even greater role in global climate interactions than we present here. More importantly, we suggest that accurate representation of dust should be a consideration in efforts to reduce monsoon biases in climate models, and dust may represent an important feedback in future projections of both the ASM and the regional and global ITCZs.

Data Availability

345 This work uses simulations from the Coupled Model Intercomparison Project (Phase 6; <https://www.wcrp-climate.org/wgcm-cmip>, World Climate Research Program, 2020). Model outputs are available on the Earth System Grid Federation (ESGF) website (<https://esgf-data.dkrz.de/search/cmip6-dkrz/>, Earth System Grid Federation, 2020).

Author Contribution

CR and LW designed the experiment; AZ carried out data processing and analysis with input from CR and LW; AZ prepared the manuscript with contributions from CR and LW.

Competing Interests

350 Laura Wilcox is a member of the editorial board.

Acknowledgements

355 This work and its contributors AZ, CLR, and LJW were supported by the UK-China Research and Innovation Partnership Fund through the Met Office Climate Science for Service Partnership (CSSP) China, DAHLIA project, as part of the Newton Fund. CLR was supported by a UK Natural Environment Research Council (NERC) independent research fellowship (grant no. NE/M018288/1). We acknowledge the World Climate Research Programme, which, through its Working Group on Coupled Modelling, coordinated and promoted CMIP6. We thank the climate modelling groups for producing and making available their model output, the Earth System Grid Federation (ESGF) for archiving the data and providing access, and the multiple funding agencies who support CMIP6 and ESGF.

360



References

- Adebiyi, A., Kok, J. F., Murray, B. J., Ryder, C. L., Stuut, J. B. W., Kahn, R. A., Knippertz, P., Formenti, P., Mahowald, N., Garcia-Pando, C. P., Klose, M., Ansmann, A., Samset, B. H., Ito, A., Balkanski, Y., Di Biagio, C., Romanias, M. N., Huang, Y., and Meng, J.: A review of coarse mineral dust in the Earth system, *Aeolian Res*, 60, 10.1016/j.aeolia.2022.100849, 2023.
- Adebiyi, A. A. and Kok, J. F.: Climate models miss most of the coarse dust in the atmosphere, *Sci Adv*, 6, 10.1126/sciadv.aaz9507, 2020.
- Aryal, Y. and Evans, S.: Dust emission response to precipitation and temperature anomalies under different climatic conditions, *Sci Total Environ*, 874, 10.1016/j.scitotenv.2023.162335, 2023.
- Aryal, Y. N. and Evans, S.: Global Dust Variability Explained by Drought Sensitivity in CMIP6 Models, *J Geophys Res-Earth*, 126, 10.1029/2021JF006073, 2021.
- Balkanski, Y., Bonnet, R., Boucher, O., Checa-Garcia, R., and Servonnat, J.: Better representation of dust can improve climate models with too weak an African monsoon, *Atmos Chem Phys*, 21, 11423-11435, 10.5194/acp-21-11423-2021, 2021.
- Carslaw, K. S., Boucher, O., Spracklen, D. V., Mann, G. W., Rae, J. G. L., Woodward, S., and Kulmala, M.: A review of natural aerosol interactions and feedbacks within the Earth system, *Atmos Chem Phys*, 10, 1701-1737, 10.5194/acp-10-1701-2010, 2010.
- Chaibou, A. A. S., Ma, X. Y., and Sha, T.: Dust radiative forcing and its impact on surface energy budget over West Africa, *Sci Rep-Uk*, 10, 10.1038/s41598-020-69223-4, 2020.
- Chen, S. Y., Huang, J. P., Qian, Y., Zhao, C., Kang, L. T., Yang, B., Wang, Y., Liu, Y. Z., Yuan, T. G., Wang, T. H., Ma, X. J., and Zhang, G. L.: An Overview of Mineral Dust Modeling over East Asia, *J Meteorol Res-Prc*, 31, 633-653, 10.1007/s13351-017-6142-2, 2017.
- Collins, W. J., Lamarque, J. F., Schulz, M., Boucher, O., Eyring, V., Hegglin, M. I., Maycock, A., Myhre, G., Prather, M., Shindell, D., and Smith, S. J.: AerChemMIP: quantifying the effects of chemistry and aerosols in CMIP6, *Geosci Model Dev*, 10, 585-607, 10.5194/gmd-10-585-2017, 2017.
- Di Biagio, C., Balkanski, Y., Albani, S., Boucher, O., and Formenti, P.: Direct Radiative Effect by Mineral Dust Aerosols Constrained by New Microphysical and Spectral Optical Data, *Geophys Res Lett*, 47, 10.1029/2019GL086186, 2020.
- Di Biagio, C., Formenti, P., Balkanski, Y., Caponi, L., Cazaunau, M., Panguì, E., Journet, E., Nowak, S., Andreae, M. O., Kandler, K., Saeed, T., Piketh, S., Seibert, D., Williams, E., and Doussin, J. F.: Complex refractive indices and single-scattering albedo of global dust aerosols in the shortwave spectrum and relationship to size and iron content, *Atmos Chem Phys*, 19, 15503-15531, 10.5194/acp-19-15503-2019, 2019.
- Dunne, J. P., Horowitz, L. W., Adcroft, A. J., Ginoux, P., Held, I. M., John, J. G., Krasting, J. P., Malyshev, S., Naik, V., Paulot, F., Shevliakova, E., Stock, C. A., Zadeh, N., Balaji, V., Blanton, C., Dunne, K. A., Dupuis, C., Durachta, J., Dussin, R., Gauthier, P. P. G., Griffies, S. M., Guo, H., Hallberg, R. W., Harrison, M., He, J., Hurlin, W., McHugh, C., Menzel, R., Milly, P. C. D., Nikonov, S., Paynter, D. J., Ploshay, J., Radhakrishnan, A., Rand, K., Reichl, B. G., Robinson, T., Schwarzkopf, D. M., Sentman, L. T., Underwood, S., Vahlenkamp, H., Winton, M., Wittenberg, A. T., Wyman, B., Zeng, Y., and Zhao, M.: The GFDL Earth System Model Version 4.1 (GFDL-ESM 4.1): Overall Coupled Model Description and Simulation Characteristics, *J Adv Model Earth Sy*, 12, 10.1029/2019MS002015, 2020.
- Evan, A. T., Flamant, C., Fiedler, S., and Doherty, O.: An analysis of aeolian dust in climate models, *Geophys Res Lett*, 41, 5996-6001, 10.1002/2014gl060545, 2014.
- Eyring, V., Bony, S., Meehl, G. A., Senior, C. A., Stevens, B., Stouffer, R. J., and Taylor, K. E.: Overview of the Coupled Model Intercomparison Project Phase 6 (CMIP6) experimental design and organization, *Geosci Model Dev*, 9, 1937-1958, 10.5194/gmd-9-1937-2016, 2016.
- Fiedler, S., Crueger, T., D'Agostino, R., Peters, K., Becker, T., Leutwyler, D., Paccini, L., Burdanowitz, J., Buehler, S. A., Cortes, A. U., Dauhut, T., Dommenges, D., Fraedrich, K., Jungandreas, L., Maher, N., Naumann, A. K., Rugenstein, M., Sakradzija, M., Schmidt, H., Sielmann, F., Stephan, C., Timmreck, C., Zhu, X. H., and Stevens, B.: Simulated Tropical Precipitation Assessed across Three Major Phases of the Coupled Model Intercomparison Project (CMIP), *Mon Weather Rev*, 148, 3653-3680, 10.1175/Mwr-D-19-0404.1, 2020.



- 410 Formenti, P., Schütz, L., Balkanski, Y., Desboeufs, K., Ebert, M., Kandler, K., Petzold, A., Scheuvs, D., Weinbruch, S., and Zhang, D.: Recent progress in understanding physical and chemical properties of African and Asian mineral dust, *Atmos Chem Phys*, 11, 8231-8256, DOI 10.5194/acp-11-8231-2011, 2011.
- Forster, P. M., Richardson, T., Maycock, A. C., Smith, C. J., Samset, B. H., Myhre, G., Andrews, T., Pincus, R., and Schulz, M.: Recommendations for diagnosing effective radiative forcing from climate models for CMIP6, *J Geophys Res-Atmos*, 121, 12460-12475, 10.1002/2016jd025320, 2016.
- 415 Froyd, K. D., Yu, P. F., Schill, G. P., Brock, C. A., Kupc, A., Williamson, C. J., Jensen, E. J., Ray, E., Rosenlof, K. H., Bian, H. S., Darmenov, A. S., Colarco, P. R., Diskin, G. S., Bui, T., and Murphy, D. M.: Dominant role of mineral dust in cirrus cloud formation revealed by global-scale measurements, *Nat Geosci*, 15, 177+, 10.1038/s41561-022-00901-w, 2022.
- Ganguly, D., Rasch, P. J., Wang, H. L., and Yoon, J. H.: Fast and slow responses of the South Asian monsoon system to anthropogenic aerosols, *Geophys Res Lett*, 39, 10.1029/2012gl053043, 2012.
- 420 Gliss, J., Mortier, A., Schulz, M., Andrews, E., Balkanski, Y., Bauer, S. E., Benedictow, A. M. K., Bian, H. S., Checa-Garcia, R., Chin, M., Ginoux, P., Griesfeller, J. J., Heckel, A., Kipling, Z., Kirkevåg, A., Kokkola, H., Laj, P., Le Sager, P., Lund, M. T., Myhre, C. L., Matsui, H., Myhre, G., Neubauer, D., van Noije, T., North, P., Olivi, D. J. L., Rémy, S., Sogacheva, L., Takemura, T., Tsigaridis, K., and Tsyro, S. G.: AeroCom phase III multi-model evaluation of the aerosol life cycle and optical properties using ground- and space-based remote sensing as well as surface in situ observations, *Atmos Chem Phys*, 21, 87-128, 10.5194/acp-21-87-2021, 2021.
- Hatzianastassiou, N., Katsoulis, B., and Vardavas, I.: Global distribution of aerosol direct radiative forcing in the ultraviolet and visible arising under clear skies, *Tellus B*, 56, 51-71, DOI 10.1111/j.1600-0889.2004.00085.x, 2004.
- 430 Hooper, J. and Marx, S.: A global doubling of dust emissions during the Anthropocene?, *Global and Planetary Change*, 169, 70-91, <https://doi.org/10.1016/j.gloplacha.2018.07.003>, 2018.
- Huang, Y., Adebisi, A. A., Formenti, P., and Kok, J. F.: Linking the Different Diameter Types of Aspherical Desert Dust Indicates That Models Underestimate Coarse Dust Emission, *Geophys Res Lett*, 48, ARTN e2020GL092054 10.1029/2020GL092054, 2021.
- Jin, Q. J., Wei, J. F., Lau, W. K. M., Pu, B., and Wang, C. E.: Interactions of Asian mineral dust with Indian summer monsoon: Recent advances and challenges (vol 215, 103562, 2021), *Earth-Sci Rev*, 216, 10.1016/j.earscirev.2021.103618, 2021.
- 435 Karydis, V. A., Tsimpidi, A. P., Bacer, S., Pozzer, A., Nenes, A., and Lelieveld, J.: Global impact of mineral dust on cloud droplet number concentration, *Atmos Chem Phys*, 17, 5601-5621, 10.5194/acp-17-5601-2017, 2017.
- Kelley, M., Schmidt, G. A., Nazarenko, L. S., Bauer, S. E., Ruedy, R., Russell, G. L., Ackerman, A. S., Aleinov, I., Bauer, M., Bleck, R., Canuto, V., Cesana, G., Cheng, Y., Clune, T. L., Cook, B., Cruz, C. A., Del Genio, A. D., Elsaesser, G. S., Faluvegi, G., Kiang, N. Y., Kim, D., Lacis, A. A., Leboissetier, A., LeGrande, A. N., Lo, K. K., Marshall, J., Matthews, E. E., McDermid, S., Mezuman, K., Miller, R. L., Murray, L. T., Oinas, V., Orbe, C., García-Pando, C. P., Perlwitz, J. P., Puma, M. J., Rind, D., Romanou, A., Shindell, D. T., Sun, S., Tausnev, N., Tsigaridis, K., Tselioudis, G., Weng, E. S., Wu, J. B., and Yao, M. S.: GISS-E2.1: Configurations and Climatology, *J Adv Model Earth Sy*, 12, 10.1029/2019MS002025, 2020.
- 440 Kirkevåg, A., Grini, A., Olivié, D., Seland, O., Alterskjær, K., Hummel, M., Karset, I. H. H., Lewinschal, A., Liu, X. H., Makkonen, R., Bethke, I., Griesfeller, J., Schulz, M., and Iversen, T.: A production-tagged aerosol module for Earth system models, *OsloAero5.3-extensions and updates for CAM5.3-Oslo*, *Geosci Model Dev*, 11, 3945-3982, 10.5194/gmd-11-3945-2018, 2018.
- 445 Kok, J. F., Ward, D. S., Mahowald, N. M., and Evan, A. T.: Global and regional importance of the direct dust-climate feedback, *Nat Commun*, 9, 10.1038/s41467-017-02620-y, 2018.
- 450 Kok, J. F., Adebisi, A. A., Albani, S., Balkanski, Y., Checa-Garcia, R., Chin, M. A., Colarco, P. R., Hamilton, D. S., Huang, Y., Ito, A., Klose, M., Li, L. L., Mahowald, N. M., Miller, R. L., Obiso, V., García-Pando, C. P., Rocha-Lima, A., and Wan, J. S.: Contribution of the world's main dust source regions to the global cycle of desert dust, *Atmos Chem Phys*, 21, 8169-8193, 10.5194/acp-21-8169-2021, 2021a.
- 455 Kok, J. F., Adebisi, A. A., Albani, S., Balkanski, Y., Checa-Garcia, R., Chin, M. A., Colarco, P. R., Hamilton, D. S., Huang, Y., Ito, A., Klose, M., Leung, D. M., Li, L. L., Mahowald, N. M., Miller, R. L., Obiso, V., García-Pando, C. P., Rocha-Lima, A., Wan, J. S., and Whicker, C. A.: Improved representation of the global dust cycle using observational constraints on dust properties and abundance, *Atmos Chem Phys*, 21, 8127-8167, 10.5194/acp-21-8127-2021, 2021b.
- Lau, K. M., Kim, M. K., and Kim, K. M.: Asian summer monsoon anomalies induced by aerosol direct forcing: the role of the Tibetan Plateau, *Clim Dynam*, 26, 855-864, 10.1007/s00382-006-0114-z, 2006.



- 460 Li, L. L., Mahowald, N. M., Miller, R. L., García-Pando, C. P., Klose, M., Hamilton, D. S., Ageitos, M. G., Ginoux, P., Balkanski, Y., Green, R. O., Kalashnikova, O., Kok, J. F., Obiso, V., Paynter, D., and Thompson, D. R.: Quantifying the range of the dust direct radiative effect due to source mineralogy uncertainty, *Atmos Chem Phys*, 21, 3973-4005, 10.5194/acp-21-3973-2021, 2021.
- Li, W. and Wang, Y. X.: Reduced surface fine dust under droughts over the southeastern United States during summertime: observations and CMIP6 model simulations, *Atmos Chem Phys*, 22, 7843-7859, 10.5194/acp-22-7843-2022, 2022.
- 465 Li, Z. Q., Lau, W. K. M., Ramanathan, V., Wu, G., Ding, Y., Manoj, M. G., Liu, J., Qian, Y., Li, J., Zhou, T., Fan, J., Rosenfeld, D., Ming, Y., Wang, Y., Huang, J., Wang, B., Xu, X., Lee, S. S., Cribb, M., Zhang, F., Yang, X., Zhao, C., Takemura, T., Wang, K., Xia, X., Yin, Y., Zhang, H., Guo, J., Zhai, P. M., Sugimoto, N., Babu, S. S., and Brasseur, G. P.: Aerosol and monsoon climate interactions over Asia, *Rev Geophys*, 54, 866-929, 10.1002/2015rg000500, 2016.
- 470 Mahowald, N. M., Kloster, S., Engelstaedter, S., Moore, J. K., Mukhopadhyay, S., McConnell, J. R., Albani, S., Doney, S. C., Bhattacharya, A., Curran, M. A. J., Flanner, M. G., Hoffman, F. M., Lawrence, D. M., Lindsay, K., Mayewski, P. A., Neff, J., Rothenberg, D., Thomas, E., Thornton, P. E., and Zender, C. S.: Observed 20th century desert dust variability: impact on climate and biogeochemistry, *Atmos Chem Phys*, 10, 10875-10893, 10.5194/acp-10-10875-2010, 2010.
- Mamalakis, A., Randerson, J. T., Yu, J. Y., Pritchard, M. S., Magnussdottir, G., Smyth, P., Levine, P. A., Yu, S., and Fofoula-Georgiou, E.: Zonally contrasting shifts of the tropical rain belt in response to climate change, *Nat Clim Change*, 11, 10.1038/s41558-020-00963-x, 2021.
- 475 Mao, R., Gong, D. Y., Kim, S. J., Zong, Q., Feng, X. Y., and Zhang, X. X.: Increasing spring dust storms in the future over the Taklimakan Desert, Northwest China: implications from changes in circulation pattern frequency in CMIP6, *Environ Res Commun*, 3, 10.1088/2515-7620/ac37ee, 2021.
- 480 Mulcahy, J. P., Johnson, C., Jones, C. G., Povey, A. C., Scott, C. E., Sellar, A., Turnock, S. T., Woodhouse, M. T., Abraham, N. L., Andrews, M. B., Bellouin, N., Browse, J., Carslaw, K. S., Dalvi, M., Folberth, G. A., Glover, M., Grosvenor, D. P., Hardacre, C., Hill, R., Johnson, B., Jones, A., Kipling, Z., Mann, G., Mollard, J., O'Connor, F. M., Palmiéri, J., Reddington, C., Rumbold, S. T., Richardson, M., Schutgens, N. A. J., Stier, P., Stringer, M., Tang, Y. M., Walton, J., Woodward, S., and Yool, A.: Description and evaluation of aerosol in UKESM1 and HadGEM3-GC3.1 CMIP6 historical simulations, *Geosci Model Dev*, 13, 6383-6423, 10.5194/gmd-13-6383-2020, 2020.
- 485 Neubauer, D., Ferrachat, S., Siegenthaler-Le Drian, C., Stier, P., Partridge, D. G., Tegen, I., Bey, I., Stanelle, T., Kokkola, H., and Lohmann, U.: The global aerosol-climate model ECHAM6.3-HAM2.3-Part 2: Cloud evaluation, aerosol radiative forcing, and climate sensitivity, *Geosci Model Dev*, 12, 3609-3639, 10.5194/gmd-12-3609-2019, 2019.
- Papadimas, C. D., Hatzianastassiou, N., Matsoukas, C., Kanakidou, M., Mihalopoulos, N., and Vardavas, I.: The direct effect of aerosols on solar radiation over the broader Mediterranean basin, *Atmos Chem Phys*, 12, 7165-7185, 10.5194/acp-12-7165-2012, 2012.
- 490 Richter, D. and Gill, T.: Challenges and Opportunities in Atmospheric Dust Emission, Chemistry, and Transport, *B Am Meteorol Soc*, 99, Es115-Es118, 10.1175/Bams-D-18-0007.1, 2018.
- Ryder, C. L.: Radiative Effects of Increased Water Vapor in the Upper Saharan Air Layer Associated With Enhanced Dustiness, *J Geophys Res-Atmos*, 126, 10.1029/2021JD034696, 2021.
- 495 Ryder, C. L., Highwood, E. J., Walser, A., Seibert, P., Philipp, A., and Weinzierl, B.: Coarse and giant particles are ubiquitous in Saharan dust export regions and are radiatively significant over the Sahara, *Atmos Chem Phys*, 19, 15353-15376, 10.5194/acp-19-15353-2019, 2019.
- Samanta, D., Karnauskas, K. B., and Goodkin, N. F.: Tropical Pacific SST and ITCZ Biases in Climate Models: Double Trouble for Future Rainfall Projections?, *Geophys Res Lett*, 46, 2242-2252, 10.1029/2018gl081363, 2019.
- 500 Samset, B. H., Myhre, G., Forster, P. M., Hodnebrog, O., Andrews, T., Faluvegi, G., Fläschner, D., Kasoar, M., Kharin, V., Kirkevåg, A., Lamarque, J. F., Olivié, D., Richardson, T., Shindell, D., Shine, K. P., Takemura, T., and Voulgarakis, A.: Fast and slow precipitation responses to individual climate forcings: A PDRMIP multimodel study, *Geophys Res Lett*, 43, 2782-2791, 10.1002/2016gl068064, 2016.
- 505 Sarangi, C., Qian, Y., Rittger, K., Leung, L. R., Chand, D., Bormann, K. J., and Painter, T. H.: Dust dominates high-altitude snow darkening and melt over high-mountain Asia, *Nat Clim Change*, 10, 1045-+, 10.1038/s41558-020-00909-3, 2020.
- Séférian, R., Nabat, P., Michou, M., Saint-Martin, D., Voltaire, A., Colin, J., Decharme, B., Delire, C., Berthet, S., Chevallier, M., Sénési, S., Franchisteguy, L., Vial, J., Mallet, M., Joetzjer, E., Geoffroy, O., Guérémy, J. F., Moine, M. P., Msadek, R., Ribes, A., Rocher, M., Roehrig, R., Salas-y-Méllia, D., Sanchez, E., Terray, L., Valcke, S., Waldman, R., Aumont, O., Bopp,



- 510 L., Deshayes, J., Éthé, C., and Madec, G.: Evaluation of CNRM Earth System Model, CNRM-ESM2-1: Role of Earth System Processes in Present-Day and Future Climate, *J Adv Model Earth Sy*, 11, 4182-4227, [10.1029/2019ms001791](https://doi.org/10.1029/2019ms001791), 2019.
- Shao, Y. P., Wyrwoll, K. H., Chappell, A., Huang, J. P., Lin, Z. H., McTainsh, G. H., Mikami, M., Tanaka, T. Y., Wang, X. L., and Yoon, S.: Dust cycle: An emerging core theme in Earth system science, *Aeolian Res*, 2, 181-204, DOI [10.1016/j.aeolia.2011.02.001](https://doi.org/10.1016/j.aeolia.2011.02.001), 2011.
- 515 Shi, L. M., Zhang, J. H., Yao, F. M., Zhang, D., and Guo, H. D.: Drivers to dust emissions over dust belt from 1980 to 2018 and their variation in two global warming phases, *Sci Total Environ*, 767, [10.1016/j.scitotenv.2020.144860](https://doi.org/10.1016/j.scitotenv.2020.144860), 2021.
- Solmon, F., Mallet, M., Elguindi, N., Giorgi, F., Zakey, A., and Konaré, A.: Dust aerosol impact on regional precipitation over western Africa, mechanisms and sensitivity to absorption properties, *Geophys Res Lett*, 35, [10.1029/2008gl035900](https://doi.org/10.1029/2008gl035900), 2008.
- Strong, J. D. O., Vecchi, G. A., and Ginoux, P.: The Response of the Tropical Atlantic and West African Climate to Saharan Dust in a Fully Coupled GCM, *J Climate*, 28, 7071-7092, [10.1175/Jcli-D-14-00797.1](https://doi.org/10.1175/Jcli-D-14-00797.1), 2015.
- 520 Sun, H., Pan, Z. T., and Liu, X. D.: Numerical simulation of spatial-temporal distribution of dust aerosol and its direct radiative effects on East Asian climate, *J Geophys Res-Atmos*, 117, [10.1029/2011jd017219](https://doi.org/10.1029/2011jd017219), 2012.
- Tegen, I., Neubauer, D., Ferrachat, S., Siegenthaler-Le Drian, C., Bey, I., Schutgens, N., Stier, P., Watson-Parris, D., Stanelle, T., Schmidt, H., Rast, S., Kokkola, H., Schultz, M., Schroeder, S., Daskalakis, N., Barthel, S., Heinold, B., and Lohmann, U.: The global aerosol-climate model ECHAM6.3-HAM2.3-Part 1: Aerosol evaluation, *Geosci Model Dev*, 12, 1643-1677, [10.5194/gmd-12-1643-2019](https://doi.org/10.5194/gmd-12-1643-2019), 2019.
- 525 Voigt, A., Pincus, R., Stevens, B., Bony, S., Boucher, O., Bellouin, N., Lewinschal, A., Medeiros, B., Wang, Z. L., and Zhang, H.: Fast and slow shifts of the zonal-mean intertropical convergence zone in response to an idealized anthropogenic aerosol, *J Adv Model Earth Sy*, 9, 870-892, [10.1002/2016ms000902](https://doi.org/10.1002/2016ms000902), 2017.
- 530 Wang, Z., Bi, L., Jia, X. J., Yi, B. Q., Lin, X. B., and Zhang, F.: Impact of Dust Shortwave Absorbability on the East Asian Summer Monsoon, *Geophys Res Lett*, 47, [10.1029/2020GL089585](https://doi.org/10.1029/2020GL089585), 2020.
- Wilcox, L. J., Dong, B., Sutton, R. T., and Highwood, E. J.: The 2014 Hot, Dry Summer in Northeast Asia, *B Am Meteorol Soc*, 96, S105-S110, [10.1175/Bams-D-15-00123.1](https://doi.org/10.1175/Bams-D-15-00123.1), 2015.
- 535 Wu, C. L., Lin, Z. H., and Liu, X. H.: The global dust cycle and uncertainty in CMIP5 (Coupled Model Intercomparison Project phase 5) models, *Atmos Chem Phys*, 20, 10401-10425, [10.5194/acp-20-10401-2020](https://doi.org/10.5194/acp-20-10401-2020), 2020.
- Wu, M. X., Liu, X. H., Yang, K., Luo, T., Wane, Z. E., Wu, C. L., Zhang, K., Yu, H. B., and Darmanov, A.: Modeling Dust in East Asia by CESM and Sources of Biases, *J Geophys Res-Atmos*, 124, 8043-8064, [10.1029/2019jd030799](https://doi.org/10.1029/2019jd030799), 2019.
- Zanis, P., Akritidis, D., Georgoulias, A. K., Allen, R. J., Bauer, S. E., Boucher, O., Cole, J., Johnson, B., Deushi, M., Michou, M., Mulcahy, J., Nabat, P., Olivie, D., Oshima, N., Sima, A., Schulz, M., Takemura, T., and Tsigaridis, K.: Fast responses on pre-industrial climate from present-day aerosols in a CMIP6 multi-model study, *Atmos Chem Phys*, 20, 8381-8404, [10.5194/acp-20-8381-2020](https://doi.org/10.5194/acp-20-8381-2020), 2020.
- 540 Zhao, A., Ryder, C. L., and Wilcox, L. J.: How well do the CMIP6 models simulate dust aerosols?, *Atmos Chem Phys*, 22, 2095-2119, [10.5194/acp-22-2095-2022](https://doi.org/10.5194/acp-22-2095-2022), 2022.
- Zhao, A. D., Stevenson, D. S., and Bollasina, M. A.: The role of anthropogenic aerosols in future precipitation extremes over the Asian Monsoon Region, *Clim Dynam*, 52, 6257-6278, [10.1007/s00382-018-4514-7](https://doi.org/10.1007/s00382-018-4514-7), 2019.
- 545 Zhao, Y., Yue, X., Cao, Y., Zhu, J., Tian, C. G., Zhou, H., Chen, Y. W., Hu, Y. H., Fu, W. J., and Zhao, X.: Multi-model ensemble projection of the global dust cycle by the end of 21st century using the Coupled Model Intercomparison Project version 6 data, *Atmos Chem Phys*, 23, 7823-7838, [10.5194/acp-23-7823-2023](https://doi.org/10.5194/acp-23-7823-2023), 2023.
- Zhou, Y. M., Wu, T. W., Zhou, Y., Zhang, J., Zhang, F., Su, X. L., Jie, W. H., Zhao, H., Zhang, Y. W., and Wang, J.: Can global warming bring more dust?, *Clim Dynam*, 61, 2693-2715, [10.1007/s00382-023-06706-w](https://doi.org/10.1007/s00382-023-06706-w), 2023.
- 550